Molecularly Imprinted Polymers and Infrared Evanescent Wave Spectroscopy. A Chemical Sensors Approach

ARTICLE *in* ANALYTICAL CHEMISTRY · OCTOBER 1999

Impact Factor: 5.64 · DOI: 10.1021/ac990050q

Anal. Chem. **1999,** *71,* 4786−4791

Correspondence

Molecularly Imprinted Polymers and Infrared Evanescent Wave Spectroscopy. A Chemical Sensors Approach

Michael Jakusch, M. Janotta, and Boris Mizaikoff*

Institute of Analytical Chemistry, Vienna University of Technology, Getreidemarkt 9/151, A-1060 Wien, Austria

Klaus Mosbach and Karsten Haupt

Department of Pure and Applied Biochemistry, Chemical Center, Lund University, P.O. Box 124, S-22100 Lund, Sweden

First steps toward a novel chemical sensor based on a molecularly imprinted polymer as the recognition element and infrared evanescent wave spectroscopy as transduction principle are presented. Noncovalently imprinted polymer layers selective for the herbicide 2,4-dichlorophenoxyacetic acid (2,4-D) have been prepared on the surface of zinc selenide attenuated total reflection elements. Selective and reversible binding of the template to the imprinted polymer could be observed on-line by Fourier transform infrared (FT-IR) spectroscopy. Control experiments were performed with nonimprinted reference polymers and with a structurally related compound. The obtained selectivity data correlate well with those previously obtained with molecularly imprinted polymers using radioligand binding assays. This demonstrates the potential for constructing stable and selective sensors for low-molecular-weight organic substances based on FT-IR spectroscopy. Moreover, FT-IR spectroscopy is demonstrated to be a valuable tool for deeper investigation of the binding mechanism in molecularly imprinted polymers.

Chemical sensors are of increasing interest within the field of modern analytical chemistry, as demonstrated both by the number of papers published and by the diversity of approaches and techniques applied. The common principle of chemical sensors is the immediate transduction of a chemical parameter (usually the concentration of an analyte of interest) into an easily processable, such as an electrical or optical, signal. The key component of most chemical sensors is a recognition element—commonly also referred to as the "selective layer". This layer interacts with the analyte to be detected, thereby encountering a characteristic change in one of its physical properties, such as mass, refractive index, light absorbance, reduction potential, etc. The transducer part of the sensor then transforms this physical property into the final readout. While sensors with potentiometric transduction had already been described more than two decades ago, other transducers such as conductometric, thermal, mass-sensitive, and optical devices are gaining increasing importance.[1] Especially optical sensors are attractive because of their flexibility and robustness. However, signals generated by all these transducer types usually have a relatively low information content. For example, one-dimensional readouts in the case of potentiometric or refractometric sensors or weakly structured spectra from UV/vis spectrophotometric transducers by themselves provide only limited information on the composition of the sample. Hence, to achieve the desired substance specificity, highly complex chemical, biochemical, or biological systems have to be introduced as recognition elements. Due to the limited stability of biological recognition elements, biosensor devices often cannot be used longer than a few weeks or in harsh environments, although in principle, they are very attractive for continuous process or environmental monitoring.

To overcome these general limitations, two strategies are possible: (i) the use of "intelligent" transducer mechanisms, which generate signals with a higher inherent information content, or (ii) the use of recognition elements exhibiting improved stability together with a pronounced chemical selectivity.

For sensing of organic compounds, one way to realize the first approach is to exploit the high molecular specificity of spectra obtained from organic molecules in the mid-infrared spectral region (MIR; 3500−500 cm^{-1}). It has already been shown that by combining MIR spectroscopy with fiber optics and evanescent wave sensing techniques (EWS), highly selective sensor systems can be realized.[2−5]

(1) Janata, J.; Josowicz, M.; Vanysek, P.; DeVaney, D. M. *Anal. Chem.* **1998**, *70*, 179R−208R.

(2) Krska, R.; Rosenberg, E.; Taga, K.; Kellner, R.; Messica, A.; Katzir, A. *Appl. Phys. Lett.* **1992**, *61* (15), 1778−1780.

10.1021/ac990050q CCC: $18.00
Published on Web 09/09/1999

For the latter strategy, molecularly imprinted polymers[6,7] (MIPs) are promising materials, since they exhibit recognition properties comparable to biological receptors, while being considerably more stable. However, to date only a few applications of MIPs in the field of chemical sensors are described in the literature.[8−15]

Clearly, a combination of both approaches, i.e., MIR-EWS sensors and molecularly imprinted polymers, will only result in improved specificity of the sensor system if the selectivity patterns of both methods are orthogonal,[1] since otherwise just the disadvantages of both systems would be introduced. In the case of MIPs, the spatial arrangement of different types of interacting groups relative to the target molecule is the most important factor for selective interaction. The characteristic IR spectrum of a compound is determined by the presence of distinct functional moieties and in the fingerprint region by the structure of the entire molecule. Due to these differences in the basic mechanisms of their molecular selectivities, it is likely that both methods will provide complementary information, thus mutually enhancing the recognition power. Hence, this combination may allow one to address analytical problems, where the selectivity of one method alone is not sufficient. For example, this may be the case when samples with complex matrixes are investigated, which would cause spectral interferences, or when structurally very similar analytes are present, which cannot easily be discriminated by a MIP alone.

The aim of this first study was to estimate the potential and limitations of a new type of chemical sensor based on molecularly imprinted polymers as the recognition element and IR evanescent wave spectroscopy as the transducer system. As a model analyte, the herbicide 2,4-dichlorophenoxyacetic acid (2,4-D) was chosen, since imprinted polymer-based assays have recently been developed for that substance.[16a]

EXPERIMENTAL SECTION

Chemicals. 2,4-Dichlorophenoxyacetic acid and phenoxyacetic acid (POAc) were from Sigma (St. Louis, MO). 2,2′-Azobis(2,4-dimethylvaleronitrile) (ABDV) was from Wako (Osaka, Japan). 4-Vinylpyridine (4-VP), methyl methacrylate (MMA), and ethylene glycol dimethacrylate (EGDMA) were from Aldrich (Gillingham-Dorset, UK). 4-VP was distilled prior to use. All other chemicals were of analytical grade, the solvents were of HPLC quality.

Table 1. Formulation of the Different Imprinted Polymers[a]

polymer	2,4-D	EGDMA	4-VP	MMA	ABDV	solvent (μL)
I-1	1	20	4	0	0.31	5000
I-2	1	13	4	7	0.26	4740
I-3	1	4	4	12	0.22	3300

[a] All amounts are in millimoles, except for the solvent. The solvent is a mixture of methanol and water (4:1; v/v).

Fourier Transform Infrared (FT-IR) Spectroscopy. Spectra were recorded on Bruker IFS66 and Vector 22 FT-IR spectrometers equipped with MCT detectors. A total of 100 scans were coadded for each spectrum. For measurements in transmission mode, standard KBr-pellets were prepared, while for attenuated total reflectance (ATR) measurements, a Perkin-Elmer ATR accessory in combination with zinc selenide (ZnSe) ATR elements (trapezoid, 50 × 10 × 2 mm, 45°) and a home-built stainless steel flow cell was used. In the latter case, a cutoff filter at 1900 cm^{-1} was used in order to enhance the signal-to-noise ratio in the relevant part of the spectrum.

Preparation of Imprinted Bulk Polymers. The composition of the different imprinted polymers is shown in Table 1. Functional and filling monomers, EGDMA as cross-linker, and methanol/water 4:1 (v/v) as porogenic solvent, as well as the template 2,4-D and ABDV as polymerization initiator, were added into a glass tube. The mixture was degassed by sonication, purged with nitrogen, and kept at 45 °C overnight. The resulting polymer monolith was ground in an electrical mortar and wet sieved through a 25-μm sieve. The polymer particles were washed twice with methanol/acetic acid 4:1 (v/v) and twice with methanol, each time by a 2-h incubation followed by centrifugation. The particles were then suspended in acetone and repeatedly sedimented for 2 h to remove coarse particles. Polymer particles from the combined supernatants were centrifuged and dried in a vacuum. Reference polymers were prepared in exactly the same way without the addition of the template 2,4-D.

To determine the binding characteristics of the imprinted polymers, radioligand binding assays were performed as outlined in ref 16: 50 mg of MIP and of reference polymer, respectively, were suspended in 5 mL of phosphate buffer (pH 7; 25 mM). Test solutions of 1 mL each were prepared by mixing 0−500 μL of these polymer suspensions, 100 μL of detergent for better wetability of the polymer particles (Triton X-100−0.1% in H_2O), 100 μL of [^{14}C]-2,4-D solution (0.26 nmol), and phosphate buffer.

Preparation of MIP Films on ATR Crystals. Polymerization solution I-2 (see Table 1) was sonicated and sparged with nitrogen. A 20-μL aliquot of the solution was pipetted onto a ZnSe ATR crystal and covered with a microscope glass slide under nitrogen atmosphere. Both parts were pressed together with spring clamps and placed in an oven at 50 °C for 3 h. Following polymerization, the ATR crystal carrying the polymer film was separated from the glass slide and could be used over several weeks without noticeable degradation. Nonimprinted control films (C-2) were

(3) Mizaikoff, B.; Göbel, R.; Krska, R.; Taga, K.; Kellner, R.; Tacke, M.; Katzir, A. *Sens. Actuators B* **1995**, *29*, 58−63.
(4) Jakusch, M.; Mizaikoff, B.; Kellner, R.; Katzir, A. *Sens. Actuators B* **1997**, *38−39*, 83−87.
(5) Regan, F.; Meaney M.; Vos. J. G.; MacCraith, B. D.; Walsh, J. E. *Anal. Chim. Acta* **1996**, *334*, 85−92.
(6) Wulff, G. *Angew. Chem., Int. Ed. Engl.* **1995**, *34*, 1812−1832.
(7) Mosbach, K.; Ramström, O. *Biotechnology* **1996**, *14*, 163−170.
(8) Haupt, K.; Mosbach, K. *Biochem. Soc. Trans.* **1998**, *27*, 344−350.
(9) Hedborg, E.; Winquist, F.; Lundström, I.; Andersson, L. I.; Mosbach, K. *Sens. Actuators A* **1993**, *37−38*, 796−799.
(10) Piletsky, S. A.; Parhometz, Y. P.; Lavryk, N. V.; Panasyuk, T. L.; El'skaya, A. V. *Sens. Actuators B* **1994**, *18−19*, 629−631.
(11) Kriz, D.; Ramström, O.; Svensson, A.; Mosbach, K. *Anal. Chem.* **1995**, *67*, 2142−2144.
(12) Kriz, D.; Kempe, M.; Mosbach, K. *Sens. Actuators B* **1996**, *33*, 178−181.
(13) Levi, R.; McNiven, S.; Piletsky, S. A.; Cheong, S. H.; Yano, K.; Karube, I. *Anal. Chem.* **1997** *69*, 2017−2021.
(14) Dickert, F. L.; Hayden, O. *TrAC, Trends Anal. Chem.* **1999**, *18* (3), 192−199.
(15) Yano, K.; Karube, I. *TrAC, Trends Anal. Chem.* **1999**, *18* (3), 199−204.
(16) (a) Haupt, K.; Dzgoev, A.; Mosbach, K. *Anal. Chem.* **1998**, *70*, 628−631. (b) Haupt, K. *React. Funct. Polym.* **1999**, *41*, 125−131.

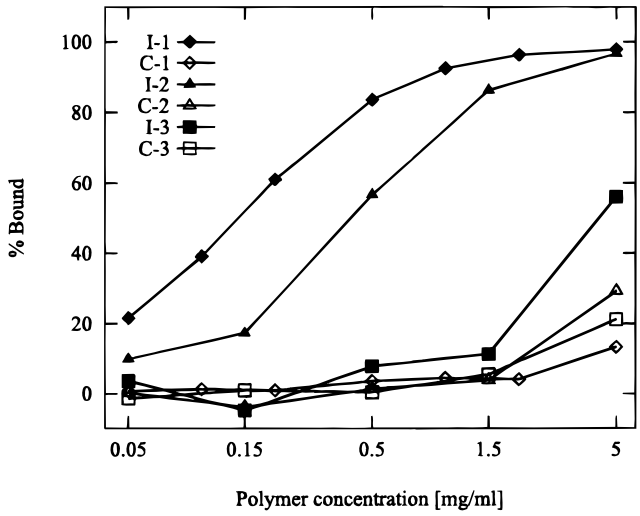

Figure 1. Percentage of bound [^{14}C]-2,4-D after incubation with suspensions of imprinted (I-1−I-3) and corresponding control (C-1−C-3) polymers. Conditions: 20 mM sodium phosphate buffer, pH 7, and 0.1% Triton X-100.

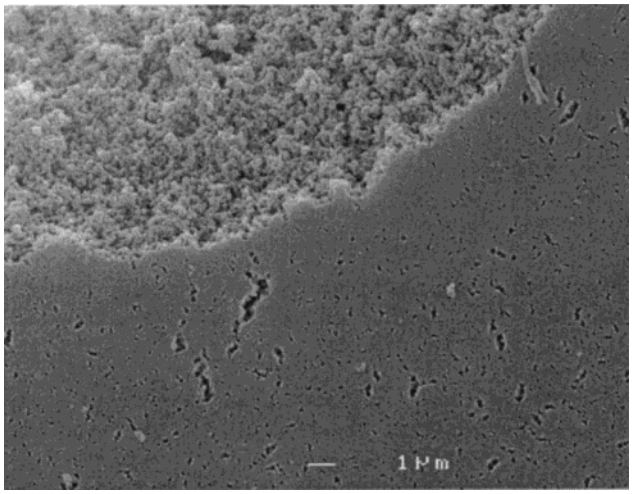

Figure 2. SEM image of a MIP layer on glass. In the upper left part of the image, the surface of the polymer layer was mechanically removed.

prepared in the same way without the addition of 2,4-D. For determining the layer thickness, scratches were made in the polymer layers and the heights of the resulting steps were measured with a profilometer (Sloan Dektak IIa).

IR−ATR Experiments. MIP-coated ATR crystals were mounted into the flow cell and sample solutions were pumped through the cell using a peristaltic pump. Prior to the adsorption experiments, the polymer layer was equilibrated with 25 mM phosphate buffer (pH 7) for 60 min. For analysis, analyte solutions in the same buffer (0.0045−4.5 mM) were pumped through the cell at a flow rate of 1.5 mL/min and spectra were recorded in 1-min intervals.

Scanning Electron Microscopy (SEM). Polymer films were prepared in exactly the same way as for the IR−ATR experiments, except that instead of the ATR crystal a glass slide was used as substrate. After polymerization, the slide was broken into small pieces in order to fit into the sample holder of the SEM (JEOL 6400; acceleration voltage, 20 kV).

RESULTS AND DISCUSSION

Imprinted Polymers. In the 2,4-D-specific imprinted polymer described in ref 16, the cross-linker content was 83% of the total monomer content (polymer I-1), yielding a hard and brittle polymer. It was observed in preliminary experiments that such a high degree of cross-linking caused problems due to the formation of cracks in thin polymer films. Therefore, polymers with lower degrees of cross-linking, namely, 50 (polymer I-2) and 20% (polymer I-3), were investigated with respect to their analyte-binding properties. To lower the degree of cross-linking, part of the EGDMA was substituted with MMA as inert filling monomer (Table 1). Figure 1 shows a titration experiment of a solution of radiolabeled 2,4-D with the imprinted and control polymers. As can be seen, the 83% and the 50% cross-linked polymers show high binding of the radioligand, whereas the corresponding control polymers bind considerably less. The 20% cross-linked polymer exhibits only poor binding of the analyte. The 50% cross-linked polymers seemed to be a good compromise and were therefore used in all experiments to prepare thin films on ATR substrates.

Polymer Coating of ATR Substrates. When we attempted to prepare thin films of MIPs on ATR substrates, problems were encountered due to the low viscosity of the monomer mixture. Standard coating procedures such as dip- or spin-coating were therefore considered not suitable. In addition, oxygen had to be excluded during polymerization. Consequently, a procedure with the polymerization carried out between the ATR crystal and a plane glass cover was chosen. In most cases, after polymerization the film adhered to the ATR element and separated well from the glass slide. The mean thickness of so prepared polymer films varied between 4 and 9 μm, and the relative standard deviation within one layer was ∼20%.

Figure 2 shows a SEM image of a MIP layer; in the upper left corner a part of a scratch is visible, which had been made into the surface in order to get also an impression of the inner structure of the polymer film. The porous structure with pore sizes between 100 nm and 1 μm is easily recognizable.

Since the preparation of homogeneous planar MIP layers turned out to be a crucial point, this step has to be considered currently a limitation for the practical application as sensing layer, which has to be further improved and optimized.

IR−ATR Experiments. Upon exposure to the test solutions, enrichment of the analyte substances in the MIP layer could be observed spectroscopically. To record time-dependent absorption curves, several bands in the analyte spectra were integrated (Figure 3). Saturation was reached after about 15 min, and the sorption process was completely reversible by rinsing with buffer.

Despite the variation in layer thickness, the reproducibility of these measurements with different polymer films was satisfactory, with relative standard deviations of the final peak areas ranging from 7.5 to 24% for the highest and lowest concentrations, respectively. Although the mean coating thickness was in the order of the evanescent wave penetration depth (∼5 μm at 1000 cm^{-1}, if a refractive index of 1.5 is assumed for the MIP coating), no correlation between the mean layer thickness and the final peak areas could be observed, which may be due to the inhomogeneity of the layer thickness.

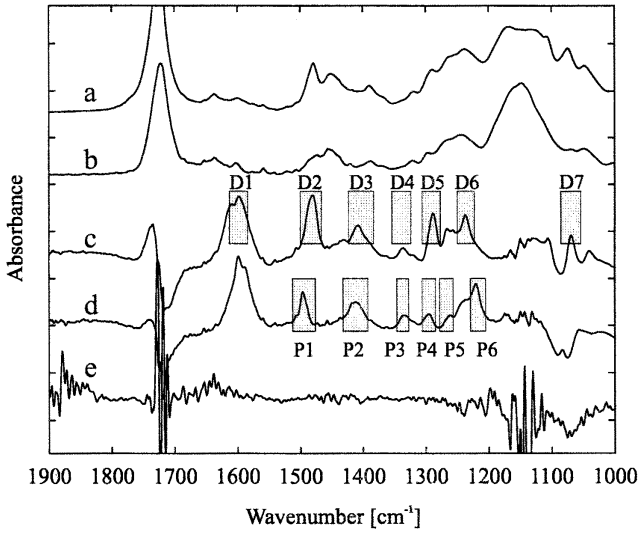

Figure 3. IR−ATR spectra of (a) the imprinted polymer I-2 before extraction of the template, (b) the control polymer C-2, spectra of (c) 2,4-D and (d) POAc adsorbed onto the imprinted polymer, and (e) a baseline spectrum obtained after equilibration of the imprinted polymer layer with buffer. The spectrum of the imprinted polymer after elution of the template did not show significant differences from the spectrum of the control polymer. The rectangles indicate the integration boundaries used for evaluation of the different absorption bands (ordinate values are scaled for better comparison).

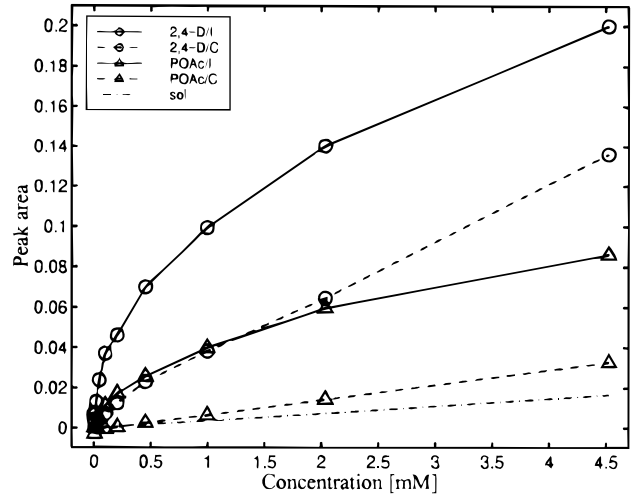

Figure 4. Sorption characteristics of 2,4-D and POAc on imprinted (I) and control (C) polymer films: Ordinate values are final peak areas after complete enrichment of the bands "D2" and "P2" for 2,4-D and POAc, respectively; "sol" indicates the signal due to free analyte solution in the active region of the evanescent field (determined by void marker experiments). Different band intensities of the respective substances were corrected for by scaling the ordinate values of "POAc" and "sol" by factors determined from measurements of aqueous solutions.

Figure 4 shows calibration curves for the binding of 2,4-D and the structurally related compound POAc to imprinted and non-imprinted polymer films. As can be seen, highest binding occurs between the template compound and the imprinted polymer. However, whereas at concentrations up to 1 mM the binding seems to follow a saturation function, at higher analyte concentrations this is overlaid by another, nonspecific adsorption, which can be attributed to partitioning of the analyte between the aqueous phase and the polymer matrix. The slope in this part of the curve is the same as for the sorption to the reference polymer, which is in accord with the assumption that nonspecific binding is identical for imprinted and corresponding reference polymers. The proportion of the absorption signal due to analyte solution in the pores of the polymer and in regions where the layer thickness is lower than the evanescent field information depth was estimated by using sodium nitrate as a nonenriched "void marker". The slope of the corresponding curve in Figure 4 is considerably smaller than for 2,4-D and POAc, indicating that the linear part of these curves is mostly really due to nonspecific binding to the respective polymers rather than being caused by the porous structure of the layers.

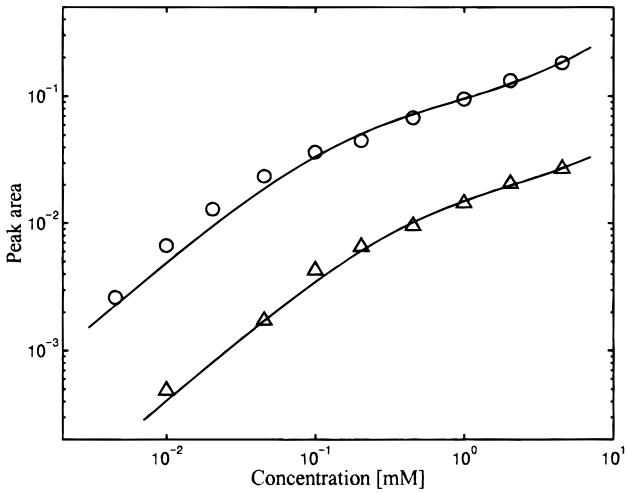

Figure 5. Experimental data and fitted sorption isotherms for 2,4-D (upper curve) and POAc (lower curve).

To quantitatively assess the sorption properties of the MIP, the experimental data were fitted to a theoretical model obtained by combining a Langmuir isotherm with a linear term:

$$y = \frac{y_{max}x}{K_D + x} + k'x$$

Although most probably a simple Langmuir model with only one dissociation constant is not sufficient to describe the sorption properties of a MIP, the quality of the fits is quite reasonable (Figure 5). Dissociation constants K_D of ~190 and ~370 μM and critical concentrations (where the signals due to specific and nonspecific binding are equal) of 4.0 and 5.5 mM for 2,4-D and POAc, respectively, were obtained. From these results, the difference between these two compounds is less pronounced than expected from the results obtained for a similar polymer,[16] which can be attributed to the lower degree of cross-linking of the polymers investigated here and to the lack of data points in the submicromolar concentration range where the polymer should exhibit higher selectivity. However, discrimination of the two substances should be easily possible due to their spectral characteristics, either by evaluating distinct absorption bands (Figure 3) or by use of chemometric techniques. Also, the determined dissociation constant for 2,4-D is about 2 orders of

Table 2. Integration Boundaries for Different Absorption Bands and Estimated Limits of Detection

key	wavenumber range (cm^{-1})	LOD (μM)	key	wavenumber range (cm^{-1})	LOD (μM)
D1	1613−1485	8.8	P1	1512−1476	50
D2	1500−1466	4.1	P2	1432−1392	12
D3	1423−1383	12	P3	1346−1327	210
D4	1354−1324	28	P4	1306−1285	37
D5	1306−1277	2.9	P5	1278−1256	170
D6	1250−1223	12	P6	1229−1205	120
D7	1085−1054	14			

magnitude larger than the one obtained with radioligand binding assays,[16b] due to the sorption effects caused by the highest affinity binding sites being currently beyond the limit of detection of our method.

From the initial slopes of the calibration functions and the standard deviation of blank measurements, limits of detection were calculated for each single absorption band (Table 2).

Since standard ATR elements have been used, high sensitivities as already reported for IR-EWS sensors[2−5,17] could not be expected. The referenced IR-EWS sensors use fiber-optics transparent in the mid-infrared region as actual sensor head. Due to the increased number of internal reflections provided by the fiber, in contrast to a conventional ATR crystal, a significantly stronger interaction of the evanescent field with the analyte is obtainable. While the preparation technique of planar molecularly imprinted polymer layers can be improved, it seems impossible to achieve an appropriate homogeneous coating of an optical fiber due to the mechanical properties of MIPs. This limitation can be circumvented with the development of planar IR transducers with a thickness of <100 μm, resulting in a substantial increase in sensitivity comparable to a sensor configuration based on optical fibers.[18,19] However, our results already show that discrimination between the structurally similar analytes 2,4-D and POAc is easily possible due to the inherent selectivity of the transducer, even though the potential of MIPs in terms of selectivity is higher at lower analyte concentrations.

Figure 6 shows spectra of 2,4-D in a KBr pellet, in aqueous buffer solution, in a dry polymer before extraction of the template, and after sorption from aqueous solution. As can be seen, in contrast to the solid state, the spectra recorded in buffer and on the imprinted polymer closely resemble each other. However, relative intensities of the bands at 1595 and 1410 cm^{-1}, which can easily be assigned to the anionic form of the carboxyl group (ν_{as} and ν_s, respectively) and the shifted bands at 1289 and 1073 cm^{-1} are different comparing dry and wet polymer film. This might be explained by two independent effects: (i) dissociation of the carboxyl group, either due to the pH or—in the case of the dry polymer and to a minor extent—ion pair formation with a pyridine ring of the polymer; and (ii) spectral changes due to solvation, which are similar in the solute and MIP-bound states.

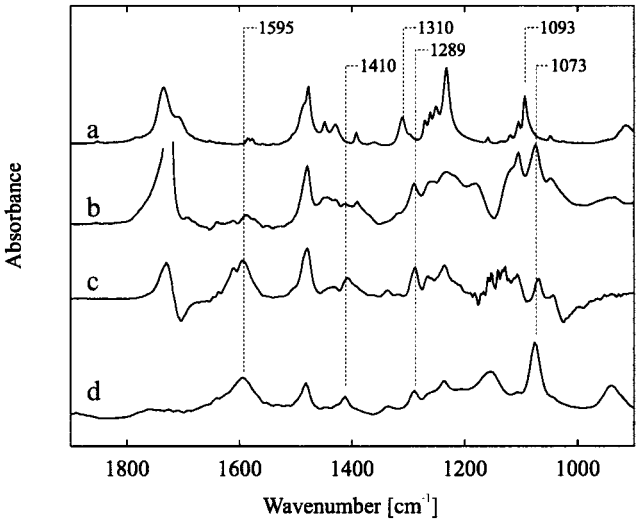

Figure 6. (a) IR reference spectrum of 2,4-D (transmission/KBr), (b) difference spectrum between an imprinted polymer before elution of the template and a control polymer, and spectra of (c) an aqueous solution of 2,4-D (c = 2 g/L, pH 7) and (d) 2,4-D adsorbed onto the imprinted polymer (ordinate values scaled). Positions where pronounced differences between the reference spectrum and the other spectra occur are denoted.

CONCLUSIONS

From these first experiments, the combination of IR-EWS sensors and MIPs appears to be a promising approach. IR spectroscopy as transducer mechanism improves the discrimination between different analytes and thus extends the scope of MIP-based sensors to applications where cross reactivities or nonspecific interactions would cause problems otherwise. Additionally, it can be expected that the combination of advanced IR-EWS transducers[2−5,17] and MIPs will lead to highly stable and selective sensor systems for the lower ppb concentration range. Methods for reproducible preparation and quality control of MIP films on IR-transparent materials are currently under investigation in our laboratories. Furthermore, MIPs sensitive for other environmentally relevant analytes, such as volatile organic compounds, are currently being developed.

The combination of optical sensor technology and molecularly imprinted polymer layers as chemical recognition element is a promising approach toward biomimetic sensors mimicking biofunctionality with the advantageous properties of polymers allowing to design enhanced monitoring schemes. Hence, new possibilities for environmental pollutant screening are enabled with the potential capability to replace conventional biosensing systems. Besides providing a considerably more robust and reliable substrate recognition layer than conventional biosensors, the unique combination of an artificial biosensing interface with an optical chemical sensor scheme will allow maximum flexibility to adopt the screening system properties for various analytes. Due to this flexibility and the particular molecular specificity of the mid-infrared region, a wide range of analytes will be addressable soon. Considering previous experiences in the field of MIPs and the potential of the presented transducer scheme, concentration ranges down to the ppb level shall be accessible sufficient for monitoring in industrial and domestic effluents, sewage plants, and surface waters.

(17) Kastner, J. F.; Tacke, M.; Katzir, A.; Edl-Mizaikoff, B.; Göbel, R.; Kellner, R. *Sens. Actuators B* **1997**, *38−39*, 163−170.
(18) Braiman, M. S.; Plunkett, S. E. *Appl. Spectrosc.* **1997**, *51*, 592−597.
(19) Plunkett, S. E.; Jonas, R. E.; Braiman, M. S. *Biophys. J.* **1997**, *73*, 2235−2240.

Apart from sensor applications, we believe that advanced IR spectroscopy could be a well-suited method to investigate the recognition of analytes by MIPs on the molecular level.

ACKNOWLEDGMENT

The authors thank Prof. Gernot Friedbacher and Elisabeth Eitenberger (Institute of Analytical Chemistry, Vienna University of Technology) for the preparation of the SEM images. Financial support by the European Commission under Project ENV4-CT97-0475 and the Austrian Federal Ministry of Science and Transport is kindly acknowledged.

Received for review January 19, 1999. Accepted July 7, 1999.

AC990050Q